Numer Algor (2017) 74:1145–1168
DOI 10.1007/s11075-016-0190-z

ORIGINAL PAPER

A meshless point collocation method for 2-D multi-term time fractional diffusion-wave equation

Rezvan Salehi[1]

Received: 14 December 2015 / Accepted: 1 August 2016 / Published online: 22 August 2016

Abstract In this paper, a meshless collocation method is considered to solve the multi-term time fractional diffusion-wave equation in two dimensions. The moving least squares reproducing kernel particle approximation is employed to construct the shape functions for spatial approximation. Also, the Caputo's time fractional derivatives are approximated by a scheme of order $O(\tau^{3-\alpha})$, $1 < \alpha < 2$. Stability and convergence of the proposed scheme are discussed. Some numerical examples are given to confirm the efficiency and reliability of the proposed method.

Keywords Multi-term time fractional diffusion-wave equation · Fractional derivatives · Caputo's derivative · Moving least squares reproducing kernel method · Meshless methods · Convergence and stability

Mathematics Subject Classification (2010) 65M70 · 65N35 · 65M15 · 65N12 · 35R11

1 Introduction

In recent years, the fractional calculus and partial differential equations of fractional orders have gained considerable attention in engineering and applied science [48, 54, 57]. Several problems in various fields of science and engineering can be modelled by fractional partial differential equations [24, 32, 64]. Unlike the local property of

✉ Rezvan Salehi
r.salehi@modares.ac.ir; rsalehi@aut.ac.ir

[1] Department of Applied Mathematics, Faculty of Mathematical Sciences, Tarbiat Modares University, P.O. Box 14115-134, Tehran, Iran

integer order derivatives, the fractional derivatives collect all of the information in a weighted form which is the so-called memory effect in science areas. Hence, there are many applications in fluid mechanics, physics, chemistry, viscoelasticity, finance, etc. [6, 21, 33, 50, 58, 60] for fractional differential equations. One can find some remarkable theoretical works on the explicit solution of fractional differential equations in [13, 27, 28, 45, 46, 68] and their references. Since the explicit solutions are available for special cases, therefore many computational efforts have been done to obtain numerical schemes for fractional differential equations. Various numerical approaches have been applied to give the approximate solution of fractional differential equations. For numerical research on fractional differential equations, one can refer to works of [16, 19, 49, 69] for finite difference solutions. The solutions by finite element method are provided in [7, 12, 25, 39, 73]. The authors of [44, 59, 66, 70, 71] are employed the spectral method to numerically solve the fractional differential equations.

In modern problems, the classical numerical approaches have been facing some difficulties due to increasing requirements for simulating complicated geometries. In these methods based on meshes, the global meshing difficulties and a large number of re-meshing in successive computational steps lead to the complexity of the computer program. Meshless methods, as alternative numerical approaches for mesh-dependent methods, have attracted much attention in the past decade. The main objective of the meshless methods is to get ride of or alleviate the difficulty of coarsening or refinement of mesh in classic methods by only adding or deleting nodes. Meshless methods may also alleviate some other problems associated with the finite element method, such as locking, element distortion and others [34, 65].

Some meshless methods have been developed, such as smoothed particle hydrodynamics (SPH) method [20], diffuse element method (DEM) [51], element-free Galerkin method (EFG) [5], reproducing kernel particle method (RKPM) [23, 35, 38], hp-clouds [15], partition of unity method (PUM) [47], meshless local Petrov–Galerkin method (MLPG) [3, 4], finite point method (FPM) [55] and so on. The meshless collocation strong form method is a truly meshless method which is easy to implement and computationally efficient.

In recent years, meshless methods based on radial basis functions (RBFs) and moving least squares (MLS) approximations are employed to numerically solve the fractional differential equations. The authors of [8] proposed a new definition of the fractional Laplacian and employed the definition for simulating the power law behaviours of three-dimensional nonlocal heat conduction by boundary-only collocation-based singular boundary method. In [43], a meshless method based on the point interpolation is developed for space fractional diffusion equations. The authors of [22] developed an implicit strong form meshless method based on RBFs approximation to numerical simulation of an anomalous subdiffusion equation. Also, they discussed the stability and convergence of the proposed scheme theoretically and numerically. In [72], the numerical solution of fractional advection-diffusion equation has been investigated by MLS-based collocation method and the stability and convergence of the method have been proven. Authors of [40, 42] proposed a numerical scheme for numerical solution of time fractional diffusion equation and fractal mobile/immobile transport model based on RBFs approximation for space

variable and a semi-discrete finite difference scheme for temporal discretization and theoretically proved the stability and convergence of the presented scheme. An implicit meshless method using MLS approximation for 2D time-dependent fractional diffusion–wave equation has been considered in [67] and analysed the stability and convergence of semi-discretized scheme related to time theoretically. Dehghan et al. [10] proposed a weak-form meshless method based on RBFs approximation for solving the time fractional reaction-subdiffusion equation and proved that the time discrete scheme is unconditionally stable and convergent using the energy method. Also, a numerical method for the solution of time fractional nonlinear sine-Gordon equation that appears extensively in classical lattice dynamics in the continuum media limit and Klein-Gordon equation which arises in physics has been presented in [9] by Kansa method [29]. The authors of [1] investigated a combination of alternating direction implicit (ADI) approach and interpolating EFG method for solving fractional reaction-subdiffusion model and obtained an error bound for the procedure using the energy method. The method of approximate particular solution is applied to constant- and variable-order time fractional diffusion model in [18]. In [17], a Laplacian transformed boundary particle method, a novel meshless method, is used to numerical modelling of time fractional diffusion equations.

In the present work, a meshless point collocation method based on the moving least squares reproducing kernel (MLSRK) approximation for spatial approximation and a finite difference approximation of order $O(\tau^{3-\alpha})$, $1 < \alpha < 2$, for Caputo's time derivatives is employed for numerical solution of multi-term time fractional diffusion-wave equation in $u(\mathbf{x}, t)$:

$$P(\partial_t)u(\mathbf{x}, t) - \Delta u(\mathbf{x}, t) = f(\mathbf{x}, t), \quad \mathbf{x} \in \Omega, \quad 0 < t \leq T, \tag{1.1}$$

$$u(\mathbf{x}, t) = h(\mathbf{x}, t), \quad \mathbf{x} \in \partial\Omega \quad 0 < t \leq T, \tag{1.2}$$

$$u(\mathbf{x}, 0) = \phi(\mathbf{x}), \quad \frac{\partial u(\mathbf{x}, 0)}{\partial t} = \psi(\mathbf{x}), \quad \mathbf{x} \in \Omega, \tag{1.3}$$

where Ω denotes a bounded and open domain in $\mathbb{R}^2$ with boundary $\partial\Omega$. The function f is the source term and initial datas, ϕ and ψ, and boundary data, $h(\mathbf{x}, t)$ are given functions on Ω. Here, the fractional operator $P(\partial t)$ is defined as

$$P(\partial_t) = \partial_t^{\alpha} + \sum_{i=1}^{m} b_i \ \partial_t^{\alpha_i}, \tag{1.4}$$

where $1 < \alpha_m \leq \cdots \leq \alpha_2 \leq \alpha_1 < \alpha < 2$ are orders of time fractional derivatives, $b_i \geq 0$, $i = 1, 2, \cdots, m$, $m \in \mathbb{N}$, are constant, and left-sided Caputo's fractional derivative, $\partial_t^{\beta} u$, $1 < \beta < 2$, is defined by [32]

$$\partial_t^{\beta} u(\mathbf{x}, t) = \frac{1}{\Gamma(2-\beta)} \int_0^t \frac{\partial^2 u(\mathbf{x}, s)}{\partial s^2} \frac{\mathrm{d}s}{(t-s)^{\beta-1}}, \quad \beta \in (1, 2), \tag{1.5}$$

where $\Gamma(.)$ denotes the gamma function.

The single-term model, the case of $m = 0$, has been employed to model many universal response of electromagnetic, acoustic and mechanical influences [31, 52, 53]. The multi-term case of model has been reported to be valuable tools to model

viscoelastic aspects, oxygen delivery through capillaries and other areas [41, 61, 62]. Numerical methods for the multi-term ordinary differential equations were studied in [30, 56]. There are a few theoretical and numerical works for model (1.1) in the literature. Applying the spectral representation of the fractional Laplacian operator, the authors of [14] converted the multi-term time-space fractional advection-diffusion equations into multi-term time fractional ordinary differential equations and by using the Luchkos theorem [46], obtained the desire analytical solution. In [26], a method of separating variables is used to solve the multi-term time fractional diffusion-wave equation in a finite domain and derived the analytical solutions of the model with three kinds of non-homogeneous boundary conditions. The authors of [2] analysed a diffusion-wave equation with two fractional derivatives of different order on bounded and unbounded spatial domains and presented a series and integral representation of the solutions. Dehghan et al. [11] employed a high order difference scheme and Galerkin spectral technique for the numerical solution of multi-term time fractional partial differential equations and stability and convergence have been proven.

The rest of this paper is organized as follows: The time discretization scheme is presented in Section 2. Also, Section 2 is devoted to prove the stability and convergence of the numerical scheme in semi-discrete form. Section 3 gives a brief discussion of the MLSRK approximation, and the numerical implementation of the proposed method is presented in the end of this section. Section 4 includes some test problems and computational results to reveal the efficiency and accuracy of the proposed method. Finally, some concluding remarks are discussed in Section 5.

2 Discrete scheme

In this section, an implicit time difference scheme for model (1.1) is suggested. Then, the stability and convergence are studied for the proposed scheme.

2.1 Derivation of time difference scheme

To obtain a time discrete scheme, the time interval $[0, T]$ is divided into N equally distance intervals of length $\tau = T/N$. For instant $t_n = n\tau$, let us define the following notations

$$u^{n-1/2} = \frac{1}{2}(u^n + u^{n-1}), \qquad \delta_t u^{n-1/2} = \frac{1}{\tau}(u^n - u^{n-1}), \tag{2.1}$$

where $u^n = u(\mathbf{x}, t_n)$. Also, let $v(\mathbf{x}, t) = \frac{\partial u(\mathbf{x},t)}{\partial t}$ and by a rewritten of the Caputo's fractional derivative (1.5), one can obtain

$$\begin{aligned} \partial_t^\alpha u(\mathbf{x}, t) &= \frac{1}{\Gamma(2-\alpha)} \int_0^t \frac{\partial^2 u(\mathbf{x}, s)}{\partial s^2} \frac{\mathrm{d}s}{(t-s)^{\alpha-1}} \\ &= \frac{1}{\Gamma(2-\alpha)} \int_0^t \frac{\partial v(\mathbf{x}, s)}{\partial s} \frac{\mathrm{d}s}{(t-s)^{\alpha-1}} = w(\mathbf{x}, t). \end{aligned} \tag{2.2}$$

Therefore, the following lemmas of [63] can be employed to approximate time fractional derivatives.

Lemma 2.1 [63]. *Suppose* $g(t) \in C^2[0, t_n]$. *Then*

$$\left| \int_0^{t_n} \frac{g'(t)}{(t_n - t)^{\beta-1}} \, \mathrm{d}t - \frac{1}{\tau} \left[a_0 g(t_n) - \sum_{k=1}^{n-1} (a_{n-k-1} - a_{n-k}) g(t_k) - a_{n-1} g(t_0) \right] \right| \leq \frac{1}{2-\beta} \left[\frac{2-\beta}{12} + \frac{2^{3-\beta}}{3-\beta} - (1 + 2^{1-\beta}) \right] \max_{0 \leq t \leq t_n} |g''(t)| \tau^{3-\beta},$$

where $a_k = \frac{\tau^{2-\beta}}{2-\beta} \left[(k+1)^{2-\beta} - k^{2-\beta} \right]$ *and* $1 < \beta < 2$.

It is obvious that $a_l > a_{l+1}$ [63]. Using above-mentioned definitions, (1.1) becomes

$$w(\mathbf{x}, t) + \sum_{i=1}^{m} b_i w_i(\mathbf{x}, t) = \Delta u(\mathbf{x}, t) + f(\mathbf{x}, t), \tag{2.3}$$

where $w_i(\mathbf{x}, t) = \partial_t^{\alpha_i} u(\mathbf{x}, t)$. Applying Taylor expansion, the following difference schemes are provided from (2.2) and (2.3)

$$v^{n-1/2} = \delta_t u^{n-1/2} + (r_1)^{n-1/2}, \tag{2.4}$$

$$w^{n-1/2} + \sum_{i=1}^{m} b_i w_i^{n-1/2} = \Delta u^{n-1/2} + f^{n-1/2} + (r_2)^{n-1/2}, \quad \mathbf{x} \in \Omega, \ n \geq 1, \tag{2.5}$$

where there exists a constant c_1 such that

$$|(r_1)^{n-1/2}| \leq c_1 \tau^2, \qquad |(r_2)^{n-1/2}| \leq c_1 \tau^2. \tag{2.6}$$

Therefore, according to Lemma 2.1, one can obtain

$$\begin{aligned} &\frac{1}{\tau \, \Gamma(2-\alpha)} \left[a_0 \delta_t u^{n-1/2} - \sum_{k=1}^{n-1} (a_{n-k-1} - a_{n-k}) \delta_t u^{k-1/2} - a_{n-1} \psi \right] \\ &+ \sum_{i=1}^{m} \frac{b_i}{\tau \, \Gamma(2-\alpha_i)} \left\{ a_{i,0} \delta_t u^{n-1/2} - \sum_{k=1}^{n-1} (a_{i,n-k-1} - a_{i,n-k}) \delta_t u^{k-1/2} - a_{i,n-1} \psi \right\} \\ &= \Delta u^{n-1/2} + f^{n-1/2} + R^{n-1/2}, \quad n \geq 1, \end{aligned} \tag{2.7}$$

where $a_{i,k} = \frac{\tau^{2-\alpha_i}}{2-\alpha_i} \left[(k+1)^{2-\alpha_i} - k^{2-\alpha_i} \right]$ and $R^{n-1/2}$ is as follows :

$$\begin{aligned} R^{n-1/2} = &- \frac{1}{\tau \Gamma(2-\alpha)} \left[a_0 (r_1)^{n-1/2} - \sum_{k=1}^{n-1} (a_{n-k-1} - a_{n-k}) (r_1)^{k-1/2} \right] \\ &- \sum_{i=1}^{m} \frac{b_i}{\tau \, \Gamma(2-\alpha_i)} \left\{ a_{i,0} (r_1)^{n-1/2} - \sum_{k=1}^{n-1} (a_{i,n-k-1} - a_{i,n-k}) (r_1)^{k-1/2} \right\} \\ &- (r_3)^{n-1/2} + (r_2)^{n-1/2} - \sum_{i=1}^{m} b_i (r_3)_i^{n-1/2}, \end{aligned}$$

where

$$|(r_3)_i^{n-1/2}| \leq c_2 \tau^{3-\alpha_i}. \tag{2.8}$$

It results from Lemma 2.1 and inequalities (2.6), (2.8) and some manipulations that

$$|R^{n-1/2}| \leq C\tau^{3-\alpha}, \tag{2.9}$$

where

$$C = \left[\frac{2c_1}{(2-\alpha)\Gamma(2-\alpha)} + c_2 + c_1 + \sum_{i=1}^{m} b_i \left\{ \frac{2c_1}{(2-\alpha_i)\Gamma(2-\alpha_i)} + c_2 \right\} \right].$$

Eventually, by eliminating the small error term, $R^{n-1/2}$, the following time difference scheme for (1.1) is obtained

$$\begin{aligned}
&\frac{1}{\tau\,\Gamma(2-\alpha)} \left[a_0 \delta_t U^{n-1/2} - \sum_{k=1}^{n-1} (a_{n-k-1} - a_{n-k}) \delta_t U^{k-1/2} - a_{n-1} \psi \right] \\
&+ \sum_{i=1}^{m} \frac{b_i}{\tau\,\Gamma(2-\alpha_i)} \left\{ a_{i,0} \delta_t U^{n-1/2} - \sum_{k=1}^{n-1} (a_{i,n-k-1} - a_{i,n-k}) \delta_t U^{k-1/2} - a_{i,n-1} \psi \right\} \\
&= \Delta U^{n-1/2} + f^{n-1/2}, \quad \mathbf{x} \in \Omega, \quad n \geq 1, \\
&U^n = h(\mathbf{x}, t_n), \quad \mathbf{x} \in \partial\Omega.
\end{aligned} \tag{2.10}$$

2.2 Analysis of semi-discrete difference scheme

In the rest of this section, the stability and convergence of the semi-discrete scheme (2.10) are proven. To this end, we introduce the following inner products and norms.

The $L^2(\Omega)$ is a Hilbert space with the inner product

$$(u, v) = \int_{\Omega} uv \, \mathrm{d}\mathbf{x}, \tag{2.11}$$

with the endowed norm

$$\|u\|_2 = (u, u)^{1/2} = \left(\int_{\Omega} u^2 \, \mathrm{d}\mathbf{x} \right)^{1/2}. \tag{2.12}$$

If we assume $\alpha = (\alpha_1, \cdots, \alpha_d)$ is a d-tuple of non-negative integers in $\mathbb{R}^d$, $|\alpha| = \sum_{i=1}^{d} \alpha_i$ and

$$D^{\alpha} u = \frac{\partial^{|\alpha|} u}{\partial x_1^{\alpha_1} \, \partial x_2^{\alpha_2} \, \cdots \partial x_d^{\alpha_d}},$$

then, one can define the Hilbert space $H^m(\Omega)$

$$H^m(\Omega) = \left\{ u \in L^2(\Omega), \;\; D^{\alpha} u \in L^2(\Omega) \text{ for all } |\alpha| \leq m \right\},$$

with inner product

$$(u, v)_m = \sum_{|\alpha|\le m} \int_\Omega D^\alpha u \, D^\alpha v \, \mathrm{d}\mathbf{x},$$

which induces the norm

$$\|u\|_{H^m(\Omega)} = \left(\sum_{|\alpha|\le m} \|D^\alpha u\|_2^2 \right)^{1/2}.$$

And, the Sobolev space $W^{1,p}(I)$ is defined as

$$W^{1,p}(\Omega) = \Big\{ u \in L^p(\Omega) | \ \exists\, g_1, g_2 \in L^p(\Omega) \text{ such that } \int_\Omega u \frac{\partial \varphi}{\partial x_i} = -\int_\Omega g_i \varphi, \ \forall \varphi \in C^1(\Omega), \ i = 1, 2 \Big\}.$$

Also, the following lemma and corollary are needed.

Lemma 2.2 [63]. *For any $G = \{G_1, G_2, \cdots\}$ and q, we have*

$$\sum_{n=1}^{N} \left[a_0 G_n - \sum_{k=1}^{n-1} (a_- a_{n-k}) G_k - a_{n-1} q \right] G_n \ge \frac{t_N^{1-\alpha}}{2} \tau \sum_{n=1}^{N} G_n^2 - \frac{t_N^{2-\alpha}}{2(2-\alpha)} q^2,$$

where a_l are defined in Lemma 2.1.

Corollary 1 *(Poincaré's inequality). Suppose that $1 \le p < \infty$ and Ω is a bounded open set. Then there exist a constant C_Ω (depending on Ω and p) such that*

$$\|u\|_{L^p(\Omega)} \le C_\Omega \|\nabla u\|_{L^p(\Omega)}, \quad \forall\, u \in W_0^{1,p}(\Omega).$$

Based on above-mentioned preliminaries, we can obtain the results of stability and convergence of time difference scheme (2.10).

Theorem 2.3 *Let U^n be the solution of discrete scheme (2.10), where as $U^n \in H_0^1(\Omega)$. Then, the time discrete scheme (2.10) is unconditionally stable in the sense that for all $\tau > 0$, the following inequality is holds*

$$\|\nabla U^n\|_2^2 \le \|\nabla U^0\|_2^2 + \sum_{j=0}^{m} \frac{b_j}{\Gamma(2-\alpha_j)} \frac{t_n^{2-\alpha_j}}{(2-\alpha_j)} \|\psi\|_2 + T t_n^{\alpha-1} \Gamma(2-\alpha) \max_{1\le k\le n} \|f^{k-1/2}\|_2^2.$$

Proof For simplicity's sake, let us put $b_0 = 1$ and $\alpha_0 = \alpha$, then time difference scheme (2.10) becomes

$$\sum_{i=0}^{m} \frac{b_i}{\tau\, \Gamma(2-\alpha_i)} \left\{ a_{i,0} \delta_t U^{n-1/2} - \sum_{k=1}^{n-1} (a_{i,n-k-1} - a_{i,n-k}) \delta_t U^{k-1/2} - a_{i,n-1} \psi \right\} = \Delta U^{n-1/2} + f^{n-1/2}.$$

Multiplying both side by $\delta_t U^{n-1/2}$ and integrating over Ω yields

$$\sum_{i=0}^{m} \frac{b_i}{\tau\,\Gamma(2-\alpha_i)} \left\{ a_{i,0}\|\delta_t U^{n-1/2}\|_2^2 - \sum_{k=1}^{n-1} (a_{i,n-k-1} - a_{i,n-k})(\delta_t U^{k-1/2}, \delta_t U^{n-1/2}) \right\}$$
$$- \sum_{i=0}^{m} \frac{b_i}{\tau\,\Gamma(2-\alpha_i)}\, a_{i,n-1}(\psi, \delta_t U^{n-1/2}) = (\Delta U^{n-1/2}, \delta_t U^{n-1/2}) + (f^{n-1/2}, \delta_t U^{n-1/2}),$$

Also, we have

$$\begin{aligned}(\Delta U^{n-1/2}, \delta_t U^{n-1/2}) &= -(\nabla U^{n-1/2}, \nabla \delta_t U^{n-1/2}) \\ &= -\int_\Omega \left(\frac{\nabla U^n + \nabla U^{n-1}}{2}\right)\left(\frac{\nabla U^n - \nabla U^{n-1}}{\tau}\right) = -\frac{1}{2\tau}\int_\Omega \left[(\nabla U^n)^2 - (\nabla U^{n-1})^2\right] \\ &= -\frac{1}{2\tau}\left(\|\nabla U^n\|_2^2 - \|\nabla U^{n-1}\|_2^2\right).\end{aligned}$$

Hence,

$$\sum_{i=0}^{m} \frac{b_i}{\tau\,\Gamma(2-\alpha_i)} \left\{ a_{i,0}\|\delta_t U^{n-1/2}\|_2^2 - \sum_{k=1}^{n-1} (a_{i,n-k-1} - a_{i,n-k})\|\delta_t U^{k-1/2}\|_2 \|\delta_t U^{n-1/2}\|_2 \right\}$$
$$- \sum_{i=0}^{m} \frac{b_i}{\tau\,\Gamma(2-\alpha_i)} a_{i,n-1}\|\psi\|_2 \|\delta_t U^{n-1/2}\|_2 \le -\frac{1}{2\tau}\left(\|\nabla U^n\|_2^2 - \|\nabla U^{n-1}\|_2^2\right)$$
$$+ \|f^{n-1/2}\|_2 \|\delta_t U^{n-1/2}\|_2.$$

Summing both side of above inequality from $n = 1$ to p, we obtain

$$\sum_{n=1}^{p}\sum_{i=0}^{m} \frac{b_i}{\tau\,\Gamma(2-\alpha_i)} \left\{ a_{i,0}\|\delta_t U^{n-1/2}\|_2 - \sum_{k=1}^{n-1} (a_{i,n-k-1} - a_{i,n-k})\|\delta_t U^{k-1/2}\|_2 - a_{i,n-1}\|\psi\|_2 \right\} \|\delta_t U^{n-1/2}\|_2$$
$$\le -\frac{1}{2\tau}\left(\|\nabla U^p\|_2^2 - \|\nabla U^0\|_2^2\right) + \sum_{n=1}^{p} \|f^{n-1/2}\|_2 \|\delta_t U^{n-1/2}\|_2.$$

Using Lemma 2.2 for left-hand side of the last inequality results in

$$\sum_{i=0}^{m} \frac{b_i}{\tau\,\Gamma(2-\alpha_i)} \left[\frac{t_p^{1-\alpha_i}}{2}\tau \sum_{n=1}^{p} \|\delta_t U^{n-1/2}\|_2^2 - \frac{t_p^{2-\alpha_i}}{2(2-\alpha_i)}\|\psi\|_2^2\right]$$
$$\le -\frac{1}{2\tau}\left(\|\nabla U^p\|_2^2 - \|\nabla U^0\|_2^2\right) + \sum_{n=1}^{p} \|f^{n-1/2}\|_2 \|\delta_t U^{n-1/2}\|_2.$$

On the other hand, using the following Young's inequality

$$|ab| \le \frac{1}{2\theta}\, a^2 + \frac{\theta}{2}\, b^2, \quad \forall \theta \ne 0,$$

with $\theta = \frac{b_0 t_p^{1-\alpha_0}}{\Gamma(2-\alpha_0)}$, we have

$$\sum_{n=1}^{p} \|f^{n-1/2}\|_2 \|\delta_t U^{n-1/2}\|_2 \le \frac{b_0 t_p^{1-\alpha_0}}{2\Gamma(2-\alpha_0)} \sum_{n=1}^{p} \|\delta_t U^{n-1/2}\|_2^2 + \frac{\Gamma(2-\alpha_0) t_p^{\alpha_0-1}}{2b_0} \sum_{n=1}^{p} \|f^{n-1/2}\|_2^2.$$

Therefore,

$$\begin{aligned} &\frac{b_0 t_p^{1-\alpha_0}}{2\Gamma(2-\alpha_0)} \sum_{n=1}^{p} \|\delta_t U^{n-1/2}\|_2^2 - \sum_{i=0}^{m} \frac{b_i t_p^{2-\alpha_i}}{2\tau(2-\alpha_i)\Gamma(2-\alpha_i)} \|\psi\|_2^2 \\ &\quad \le \frac{b_0 t_p^{1-\alpha_0}}{2\Gamma(2-\alpha_0)} \sum_{n=1}^{p} \|\delta_t U^{n-1/2}\|_2^2 + \frac{\Gamma(2-\alpha_0) t_p^{\alpha_0-1}}{2b_0} \sum_{n=1}^{p} \|f^{n-1/2}\|_2^2 \\ &\qquad - \frac{1}{2\tau} \left(\|\nabla U^p\|_2^2 - \|\nabla U^0\|_2^2 \right). \end{aligned}$$

Multiplying both side by 2τ yields

$$\|\nabla U^p\|_2^2 \le \|\nabla U^0\|_2^2 + \sum_{i=0}^{m} \frac{b_i t_p^{2-\alpha_i}}{(2-\alpha_i)\Gamma(2-\alpha_i)} \|\psi\|_2^2 + \frac{\tau\Gamma(2-\alpha_0) t_p^{\alpha_0-1}}{b_0} \sum_{n=1}^{p} \|f^{n-1/2}\|_2^2.$$

Then, we can obtain

$$\|\nabla U^p\|_2^2 \le \|\nabla U^0\|_2^2 + \sum_{i=0}^{m} \frac{b_i t_p^{2-\alpha_i}}{(2-\alpha_i)\Gamma(2-\alpha_i)} \|\psi\|_2^2 + T\,\Gamma(2-\alpha) t_p^{\alpha-1} \max_{1\le k\le p} \|f^{k-1/2}\|_2^2.$$

Finally, changing index from p to n, we have

$$\|\nabla U^n\|_2^2 \le \|\nabla U^0\|_2^2 + \sum_{i=0}^{m} \frac{b_i t_n^{2-\alpha_i}}{(2-\alpha_i)\Gamma(2-\alpha_i)} \|\psi\|_2^2 + T\,\Gamma(2-\alpha) t_n^{\alpha-1} \max_{1\le k\le n} \|f^{k-1/2}\|_2^2,$$

which is complete the proof. □

Theorem 2.4 *Let $u^n = u(\mathbf{x}, t_n) \in H_0^1$ be the exact solution of (2.7) and U^n be its approximate solution from (2.10), then the time difference scheme (2.10) is convergent with convergence order $O(\tau^{3-\alpha})$.*

Proof We set

$$e^n = u^n - U^n, \quad n \geq 1,$$

where $e_0 = 0$. Subtracting (2.7) form (2.10), the following error equation is obtained

$$\begin{aligned}
&\frac{1}{\tau\,\Gamma(2-\alpha)}\left[a_0\delta_t e^{n-1/2} - \sum_{k=1}^{n-1}(a_{n-k-1} - a_{n-k})\delta_t e^{k-1/2}\right] \\
&+ \sum_{i=1}^{m}\frac{b_i}{\tau\,\Gamma(2-\alpha_i)}\left\{a_{i,0}\delta_t e^{n-1/2} - \sum_{k=1}^{n-1}(a_{i,n-k-1} - a_{i,n-k})\delta_t e^{k-1/2}\right\} \\
&= \Delta e^{n-1/2} + R^{n-1/2}.
\end{aligned}$$

Using the obtained results in the stability Theorem 2.3, we have

$$\|\nabla e^n\|_2^2 \leq \tau\Gamma(2-\alpha)t_n^{\alpha-1}\sum_{k=1}^{n}\|R^{k-1/2}\|_2^2.$$

By inserting (2.9) into the right-hand side of the last inequality, we can obtain

$$\|\nabla e^n\|_2 \leq C\sqrt{T^\alpha\Gamma(2-\alpha)}\,\tau^{3-\alpha}.$$

Now, using Poincaré's inequality form Corollary 1, we have

$$\|e^n\|_2 \leq C_\Omega\, C\sqrt{T^\alpha\Gamma(2-\alpha)}\,\tau^{3-\alpha},$$

which is complete the proof. □

3 The MLSRK approximation and full discretization

In the current work, the spatial discretization is constructed by moving least squares reproducing kernel (MLSRK) approximation [36, 37]. The MLSRK approximation was provided as a different version of the moving least squares (MLS) approximation where the shape functions are generated by a local least squares approach. The interpolation of this kind contains a reproducing kernel (RK), which, as a generalization of the discrete case, establishes a continuous basis for a partition of unity and can reproduce any smooth function accurately in a global least squares sense.

Let $u(x)$, $x \in \mathbb{R}^d$, be a sufficiently smooth function defined on a simply open set $\Omega \subset \mathbb{R}^d$ with a Lipschitz continuous boundary. For each $x \in \overline{\Omega}$, we define

$$\mathcal{B}(x) = \{y \in \Omega |\, \varphi(\frac{x-y}{\rho}) \neq 0\} \subseteq \Omega. \tag{3.1}$$

Also, for a positive integer q, the space of polynomials of degree less than or equal to q in $\mathbb{R}^d$ is defined as

$$\mathcal{P}_{q,d} = \text{span}\{(x-y)^\alpha\}_{\alpha:\,|\alpha|\leq q}, \tag{3.2}$$

and define $u_x : \mathcal{B}(x) \to \mathbb{R}$ by

$$u_x(y) = u(y), \quad \forall y \in \mathcal{B}(x). \tag{3.3}$$

The global approximation $u^G : \Omega \to \mathbb{R}$ is obtained as follows

$$u^G(x) := \lim_{\bar{x}\to x} (L_{\bar{x}}u)(x), \qquad \forall x \in \overline{\Omega}. \tag{3.4}$$

where $L_{\bar{x}}u : \mathcal{B}(\bar{x}) \to \mathbb{R}$ is a local approximant for function $u_{\bar{x}} : \Omega \to \mathbb{R}$. In the current contribution, for a fixed point $\bar{x} \in \bar{\Omega}$, the local approximant is considered as follows:

$$u^l(x) = (L_{\bar{x}}u)(x) := \sum_{i=1}^{Q} \psi_i(\frac{x-\bar{x}}{\rho}) d_i(\bar{x}) = \Psi(\frac{x-\bar{x}}{\rho})\mathbf{d}(\bar{x}), \tag{3.5}$$

where $Q = \dim \mathcal{P}_{q,d} = \begin{pmatrix} q+d \\ d \end{pmatrix}$ and

$$\mathbf{d}^t(y) := \{d_1, d_2, \cdots, d_Q\}(x), \tag{3.6}$$

$$\Psi(y) := \{p_1, p_2, \cdots, p_Q\}, \tag{3.7}$$

$$p_i = \frac{(x-y)^{\alpha_i}}{\rho}, \quad i = 1, 2, \cdots, q. \tag{3.8}$$

Since the polynomial series is finite, then we can define a residual r_ρ

$$r_\rho := u^l(x) - \Psi(\frac{x-\bar{x}}{\rho})\mathbf{d}(\bar{x}), \quad x \in \mathcal{B}(\bar{x}). \tag{3.9}$$

Then, a functional related to this residual is defined as

$$\mathcal{J}(\mathbf{d}(\bar{x})) = \int_{\mathcal{B}(\bar{x})} r_\rho^2(x, \bar{x})\omega_\rho(x-\bar{x})\, \mathrm{d}\mathcal{B}, \tag{3.10}$$

where $\omega_\rho(x-\bar{x}) = \omega(\frac{x-\bar{x}}{\rho})$. One can obtain the following equation by minimizing the quadratic form $\mathcal{J}(\mathbf{d}(\bar{x}))$

$$\int_{\mathcal{B}(\bar{x})} \Psi^t(\frac{x-\bar{x}}{\rho}) \left(u^l(x) - \Psi(\frac{x-\bar{x}}{\rho})\mathbf{d}(\bar{x}) \right) \omega_\rho(x-\bar{x})\, \mathrm{d}\mathcal{B} = 0. \tag{3.11}$$

When $\mathrm{supp}\{\omega_\rho(x-\bar{x})\} \subseteq \overline{\mathcal{B}}$, then the above integral can be extended over the whole domain

$$\int_{\Omega_x} \Psi^t(\frac{x-\bar{x}}{\rho}) \left(u^l(x) - \Psi(\frac{x-\bar{x}}{\rho})\mathbf{d}(\bar{x}) \right) \omega_\rho(x-\bar{x})\, \mathrm{d}\Omega_x = 0, \tag{3.12}$$

which yields

$$\left(\int_{\Omega_x} \Psi^t(\frac{x-\bar{x}}{\rho})\omega_\rho(x-\bar{x})\Psi(\frac{x-\bar{x}}{\rho})\mathrm{d}\,\Omega_x \right) \mathbf{d}(\bar{x}) = \int_{\Omega_x} \Psi^t(\frac{x-\bar{x}}{\rho})u(x)\omega_\rho(x-\bar{x})\mathrm{d}\,\Omega_x. \tag{3.13}$$

Now, if we define the moment matrix $\mathcal{M}(x)$ as follows

$$\mathcal{M}(\bar{x}) := \int_{\Omega_x} \Psi^t(\frac{x-\bar{x}}{\rho})\omega_\rho(x-\bar{x})\Psi(\frac{x-\bar{x}}{\rho})\, \mathrm{d}\Omega_x, \tag{3.14}$$

then the unknown vector $\mathbf{d}(\bar{x})$ is determined as

$$\mathbf{d}(\bar{x}) = \mathcal{M}^{-1}(\bar{x}) \int_{\Omega_x} \Psi^t(\frac{x-\bar{x}}{\rho}) u(x) \omega_\rho(x-\bar{x})\, \mathrm{d}\Omega_x. \tag{3.15}$$

According to (3.5) and (3.15), we will have

$$\begin{aligned} u^l(x) = (L_{\bar{x}}u)(x) &= \Psi(\frac{x-\bar{x}}{\rho})\mathbf{d}(\bar{x}) \\ &= \Psi(\frac{x-\bar{x}}{\rho})\mathcal{M}^{-1}(x) \int_{\Omega_y} \Psi^t(\frac{y-\bar{x}}{\rho}) u(y) \omega_\rho(y-\bar{x})\, \mathrm{d}\,\Omega_y \quad \forall x \in \mathcal{B}(\bar{x}). \end{aligned} \tag{3.16}$$

So, according to relation (3.4), the global approximant function $u^G : \Omega \to \mathbb{R}$, is obtained in the following form

$$u^G(x) = (L_x u)(x) = \Psi(0)\mathcal{M}^{-1}(x) \int_{\Omega} \Psi^t(\frac{y-x}{\rho}) u(y) \omega_\rho(y-x)\, \mathrm{d}\,\Omega, \quad \forall x \in \Omega. \tag{3.17}$$

Now, we set

$$\mathcal{C}_\rho(x, x-y) = \Psi(0)\mathcal{M}^{-1}(x)\Psi^t(\frac{y-x}{\rho}). \tag{3.18}$$

Substituting (3.18) into (3.17), gives

$$u^G(x) = \int_{\Omega} \mathcal{C}_\rho(x, x-y) u(y) \omega_\rho(y-x)\, \mathrm{d}\,\Omega, \quad \forall x \in \Omega. \tag{3.19}$$

Let

$$\mathcal{K}_\rho(x, x-y) = \mathcal{C}_\rho(x, x-y)\omega_\rho(y-x), \tag{3.20}$$

where the function $\mathcal{K}_\rho$ is the so-called reproducing kernel function. Therefore, we will have

$$u(x) := \int_{\Omega} \mathcal{K}_\rho(x, x-y) u(y)\, \mathrm{d}\,\Omega. \tag{3.21}$$

In order to use (3.21) in the numerical approximation, the integral must be discretized. Let $\{x_i\}_{i=1}^{NP}$, be an admissible particle distribution [36], then by employing the numerical quadrature, one can approximate (3.21) as follows:

$$\begin{aligned} u_h(x) &= \sum_{i=1}^{NP} u(x_i)\mathcal{C}_\rho^h(x, x_i - x)\omega_\rho(x_i - x)\Delta V_i \\ &= \sum_{i=1}^{NP} \mathcal{K}_\rho^h(x, x_i - x) u_i \Delta V_i, \end{aligned} \tag{3.22}$$

where ΔV_i is the quadrature weights or ith particle lumped volume and

$$\mathcal{C}_\rho^h(x, y-x) = \Psi(0)(\mathcal{M}^h)^{-1}(x)\Psi^t(\frac{y-x}{\rho}), \tag{3.23}$$

where

$$\mathcal{M}^h(x) = \sum_{i=1}^{NP} \Psi^t(\frac{x_i - x}{\rho})\omega_\rho(x_i - x)\Psi(\frac{x_i - x}{\rho})\Delta V_i. \tag{3.24}$$

Now, (3.21) can be written as

$$u_h(x) = \sum_{i=1}^{NP} \Phi_i(\rho, x, x_i) u_i, \tag{3.25}$$

where

$$\Phi_i(\rho, x, x_i) = \mathcal{C}_\rho^h(x, x_i - x)\omega_\rho(x_i - x)\Delta V_i, \tag{3.26}$$

$$= \Psi(0)(\mathcal{M}^h)^{-1}(x)\Psi^t(\frac{x_i - x}{\rho})\omega_\rho(x_i - x)\Delta V_i \tag{3.27}$$

$$= \mathcal{K}_\rho^h(x, x_i - x)\Delta V_i. \tag{3.28}$$

In the rest of this section, the full discrete scheme for model problem (1.1) is obtained by inserting the MLSRK approximation (3.26) as spatial approximation in semi discrete scheme (2.10). Applying strong form, the point collocation meshless method yields a system of discretized equations for nodes inside the domain and on essential boundary. Approximating $U^n = U(\mathbf{x}, t_n)$ as (3.26), substituting into the semi discrete scheme (2.10) and applying collocation method at each interior point $\mathbf{x}_j$, lead to

$$\frac{1}{\tau\,\Gamma(2-\alpha)}\left[a_0\delta_t U_j^{n-1/2} - \sum_{k=1}^{n-1}(a_{n-k-1} - a_{n-k})\delta_t U_j^{k-1/2} - a_{n-1}\psi_j\right]$$
$$+\sum_{i=1}^{m}\frac{b_i}{\tau\,\Gamma(2-\alpha_i)}\left\{a_{i,0}\delta_t U_j^{n-1/2} - \sum_{k=1}^{n-1}(a_{i,n-k-1} - a_{i,n-k})\delta_t U_j^{k-1/2} - a_{i,n-1}\psi_j\right\}$$
$$= \Delta U_j^{n-1/2} + f_j^{n-1/2}, \quad n \geq 1.$$

If we set

$$\mu_0 = \frac{1}{\tau^2\Gamma(2-\alpha)}, \quad \mu_i = \frac{b_i}{\tau^2\Gamma(2-\alpha_i)}, \ i = 1, 2, \cdots, m.$$

Then, we can simplify the full discrete scheme in the following form

$$[a_0\mu_0 + \sum_{i=1}^{m}\mu_i a_{i,0}]U_j^n - \frac{1}{2}\Delta U_j^n = [a_0\mu_0 + \sum_{i=1}^{m}\mu_i a_{i,0}]U_j^{n-1}$$
$$+\sum_{k=1}^{n-1}\left\{\mu_0(a_{n-k-1} - a_{n-k}) + \sum_{i=1}^{m}\mu_i(a_{i,n-k-1} - a_{i,n-k})\right\}(U_j^k - U_j^{k-1})$$
$$+[\tau\mu_0 a_{n-1} + \sum_{i=1}^{m}\tau\mu_i a_{i,n-1}]\psi_j + \frac{1}{2}\Delta U_j^{n-1} + f_j^{n-1/2}, \tag{3.29}$$

where

$$U_j^k = U(\mathbf{x}_j, k\tau) = \sum_{i=1}^{NP}\Phi_i(\rho, \mathbf{x}_j, \mathbf{x}_i)\hat{U}_i^k,$$

$$\Delta U_j^k = \sum_{i=1}^{NP}\Delta\Phi_i(\rho, \mathbf{x}_j, \mathbf{x}_i)\hat{U}_i^k.$$

Also, the essential boundary condition is imposed as

$$\sum_{i=1}^{NP} \Phi_i(\rho, \mathbf{x}_j, \mathbf{x}_i)\hat{U}_i^k = h(\mathbf{x}_j, k\tau), \quad \mathbf{x}_j \in \partial\Omega. \tag{3.30}$$

4 Numerical results

To verify the theoretical results and show the efficiency and applicability of the proposed approach, two-dimensional numerical test is solved with regular and irregular nodal points in rectangular, circular and complex domains. For this purpose, the following error indicator and convergence ratio are used

$$L_\infty(\tau) = \max_{1\le j\le NP} \left|U(\mathbf{x}_j, T) - u(\mathbf{x}_j, T)\right|,$$

and

$$\text{Ratio} = \frac{\log(\frac{L_\infty(\tau_1)}{L_\infty(\tau_2)})}{\log(\frac{\tau 1}{\tau 2})},$$

where τ_1 and τ_2 are different time step-sizes.

In the test problems, the quadratic basis ($m = 2$) and Gaussian weight function are employed as

$$w_i(\mathbf{x}) = w_\rho(\mathbf{x}_i - \mathbf{x}) = \begin{cases} \frac{\exp[-(d_i/c_i)^2]-\exp[-(r_i/c_i)^2]]}{1-\exp[-(r_i/c_i)^2]}, & 0 \le d_i \le r_i, \\ 0, & d_i > r_i, \end{cases} \tag{4.1}$$

where $d_i = \|\mathbf{x} - \mathbf{x}_i\|_2$, c_i is a constant controlling the shape of the weight function w_i and r_i is the size of the support domain of node i.

Consider the following two-dimensional multi-term time fractional diffusion-wave equation

$$\partial_t^\alpha u(x, y, t) + \partial_t^{\alpha_1} u(x, y, t) = \Delta u(x, y, t) + f(x, y, t), \tag{4.2}$$

subject to zero initial conditions and boundary conditions are generated from exact solution values on the boundary. The exact solution of this problem is

$$u(x, y, t) = \mathrm{e}^{x+y}\, t^{2+\alpha+\alpha_1}.$$

4.1 Test problem with rectangular domain

First of all, we discretize the problem domain, $\Omega = [0, 1] \times [0, 1]$, with 4096 ($64 \times 64$) regularly distributed points (see Fig. 1a). Then, the discrete scheme (3.29) is applied to solve the 2-D multi-term time fractional diffusion-wave equation. The plots of exact and approximate solutions at $t = 1$ with $\alpha = 1.3$, $\alpha_1 = 1.1$ are depicted in Fig. 2. In Table 1, the absolute error and ratio are listed. One can see that the obtained results are in a good agreement with the theoretical results since the ratios are around $(3 - \alpha)$ as we expected from theory.

Moreover, the problem domain is discretized with 4096 Halton type non-uniform irregular point distribution as shown in Fig. 1b. The approximate and exact solutions

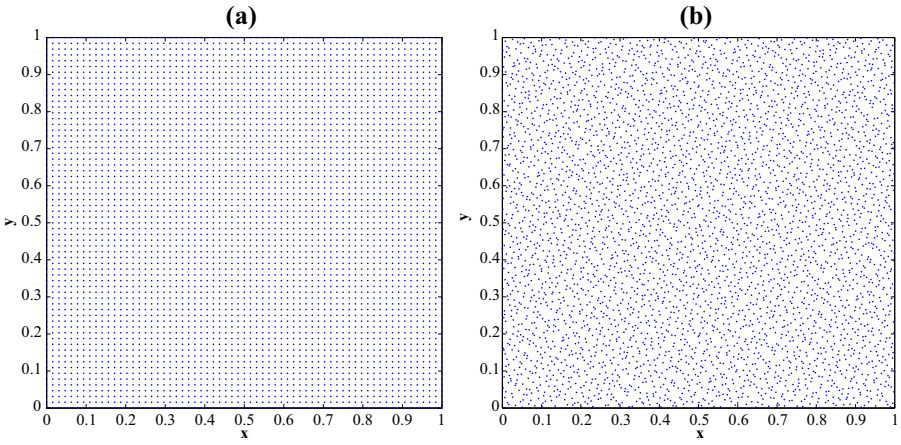

Fig. 1 **a** Regular and **b** irregular nodal distribution for rectangular domain

at $t = 1$ for $\alpha = 1.5$, $\alpha_1 = 1.3$ are plotted in Fig. 3. To verify the theoretical results associated with time step-size, the absolute error and ratios are reported in Table 2 for different step-sizes when the step-size τ decrease from $1/20$ to $1/320$. It can be seen that the error decreases with expected rate in either case.

4.2 Test problem with circular domain

As the second example, we solve the studied problem on a circular domain. Particularly, (1.1)–(1.3) are solved over the circular domain with its center at (0.5, 0.5) and

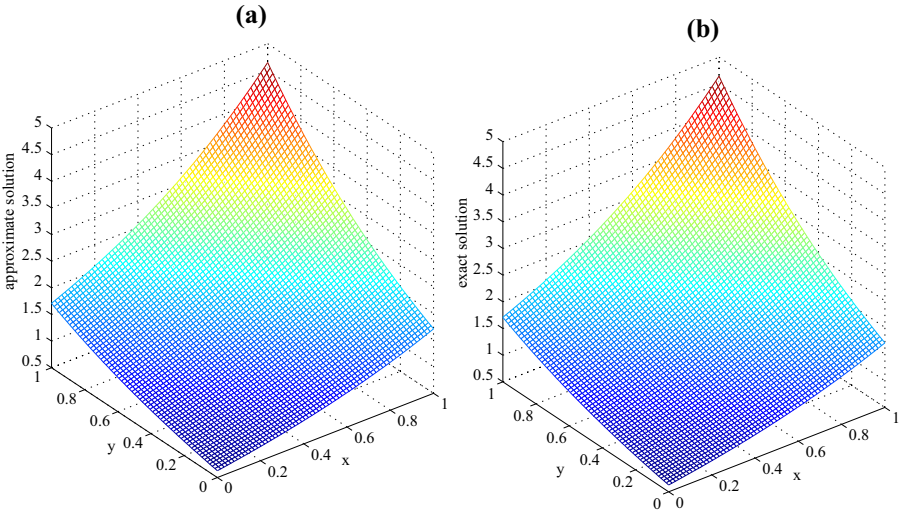

Fig. 2 Approximate and exact solutions at $t = 1$ associated with regularly distributed nodes in rectangular domain with $\alpha = 1.3$, $\alpha_1 = 1.1$

Table 1 Absolute error and convergence rate associated with different time step-size for 1089 regularly distributed nodes on rectangular domain

$\alpha = 1.3, \alpha_1 = 1.1$			$\alpha = 1.5, \alpha_1 = 1.3$		
Step-size τ	L_∞	Ratio	Step-size τ	L_∞	Ratio
1/20	8.34432×10^{-3}	–	1/20	2.80285×10^{-2}	–
1/40	2.74260×10^{-3}	1.6052	1/40	1.02452×10^{-2}	1.4519
1/80	8.69406×10^{-4}	1.6574	1/80	3.66827×10^{-3}	1.4818
1/160	2.72014×10^{-4}	1.6763	1/160	1.33058×10^{-3}	1.4630
1/320	9.16615×10^{-5}	1.5693	1/320	4.65437×10^{-4}	1.5154

radius $r = 0.5$. Firstly, the circular problem domain is discretized with 4096 irregularly distributed nodal points as shown in Fig. 4. Afterwards, we solve the studied model with proposed meshless point collocation method using irregularly distributed points for both cases $\alpha = 1.3$, $\alpha_1 = 1.1$ and $\alpha = 1.5$, $\alpha_1 = 1.3$.

The plots of exact solution versus approximate solution for $\alpha = 1.3$, $\alpha_1 = 1.1$ are figured in Fig. 5. Also, in Fig. 6, the absolute error of the obtained results is plotted. Like the rectangular case, absolute errors for both cases $\alpha = 1.3$, $\alpha_1 = 1.1$ and $\alpha = 1.5$, $\alpha_1 = 1.3$ with different time step-sizes τ are reported in Table 3. It is obvious from Table 3 that the obtained results are appropriately confirmed the theoretical outcomes on circular domain with irregularly distributed nodal points.

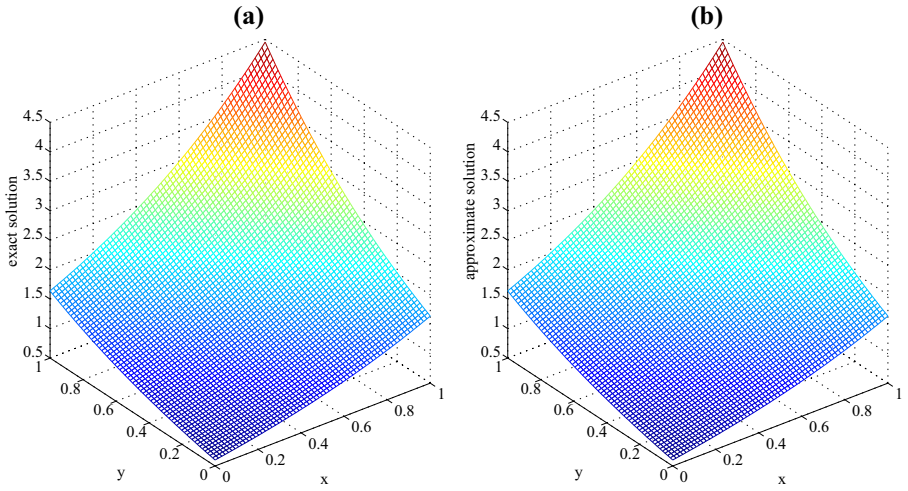

Fig. 3 Approximate and exact solutions at $t = 1$ associated with irregularly distributed nodes in rectangular domain with $\alpha = 1.5$, $\alpha_1 = 1.3$

Table 2 Absolute error and convergence rate associated with different time step-size for 1089 regularly distributed nodes on rectangular domain

$\alpha = 1.3, \alpha_1 = 1.1$			$\alpha = 1.5, \alpha_1 = 1.3$		
Step-size τ	L_∞	Ratio	Step-size τ	L_∞	Ratio
1/20	8.13847×10^{-3}	–	1/20	2.80073×10^{-2}	–
1/40	2.50628×10^{-3}	1.6992	1/40	1.02078×10^{-2}	1.4561
1/80	7.55901×10^{-4}	1.7293	1/80	3.62411×10^{-3}	1.4939
1/160	2.59268×10^{-4}	1.5437	1/160	1.28354×10^{-3}	1.4975
1/320	9.09436×10^{-5}	1.5114	1/320	4.65437×10^{-4}	1.4635

4.3 Test problem with complex domain

To test the ability of the proposed scheme to deal with complex geometries, the studied problem is considered on irregular domains as depicted in Fig. 7. The domains are generated by criterion $r = \frac{1}{n^2}\big[1 + 2n + n^2 - (n+1)\cos(n\theta)\big]$, where we used $n = 4$ and $n = 10$ to produce Ω_1 and Ω_2, respectively. After that, the problem domains are discretized with Halton type non-uniform nodal points and the problem is solved with $\alpha = 1.3$, $\alpha_1 = 1.1$.

The numerical results are reported as Figs. 8 and 9 that are shown the graphs of approximate solution and obtained absolute errors and their contour plots for $n = 4$ and $n = 10$, respectively. The depicted figures in this test and previous one are shown the reliability of the obtained results from discrete scheme and proficiency of the proposed meshless method. To figure out the convergence of proposed method for these type of geometries, absolute errors and ratios are summarized in Table 4.

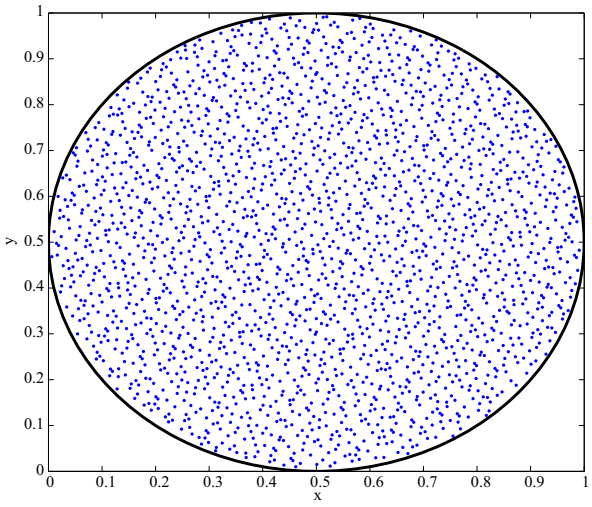

Fig. 4 Irregular nodal distribution for circular domain

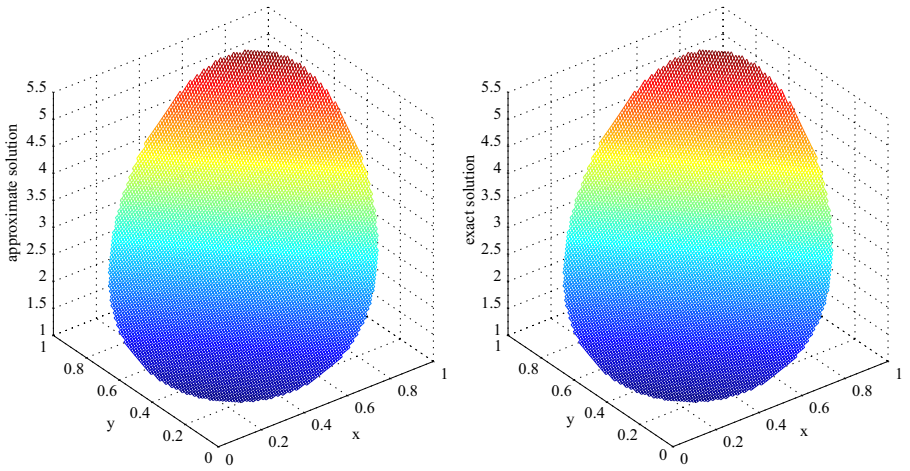

Fig. 5 Approximate and exact solutions at $t = 1$ associated with irregularly distributed nodes in circular domain with $\alpha = 1.3,\ \alpha_1 = 1.1$

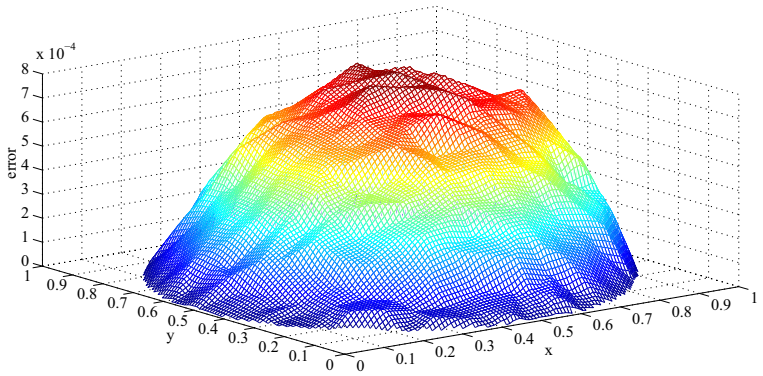

Fig. 6 Absolute error associated with irregularly distributed nodes in circular domain with $\alpha = 1.3$, $\alpha_1 = 1.1$

Table 3 Absolute error and convergence rate associated with different time step-size for 1089 irregular nodal points on circular domain

$\alpha = 1.3, \alpha_1 = 1.1$			$\alpha = 1.5, \alpha_1 = 1.3$		
Step-size τ	L_∞	Ratio	Step-size τ	L_∞	Ratio
1/20	7.23182×10^{-3}	–	1/20	2.44933×10^{-2}	–
1/40	2.44147×10^{-3}	1.5666	1/40	9.04352×10^{-3}	1.4374
1/80	9.58633×10^{-4}	1.3486	1/80	3.34827×10^{-3}	1.4335
1/160	3.67174×10^{-4}	1.3845	1/160	1.23395×10^{-3}	1.4401
1/320	1.34244×10^{-4}	1.4516	1/320	4.54384×10^{-4}	1.4413

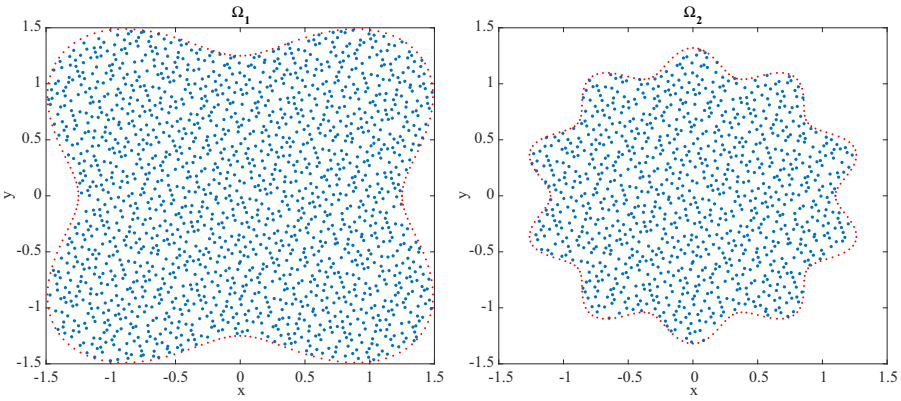

Fig. 7 The considered irregular problem domains

The obtained results suitably proved the reliability of proposed scheme for irregular domains. Also, to investigate the computational cost of implemented algorithm for the proposed method, CPU times (in seconds) for four considered domains are reported in Table 5 with different mesh-size N for irregularly distributed nodal points.

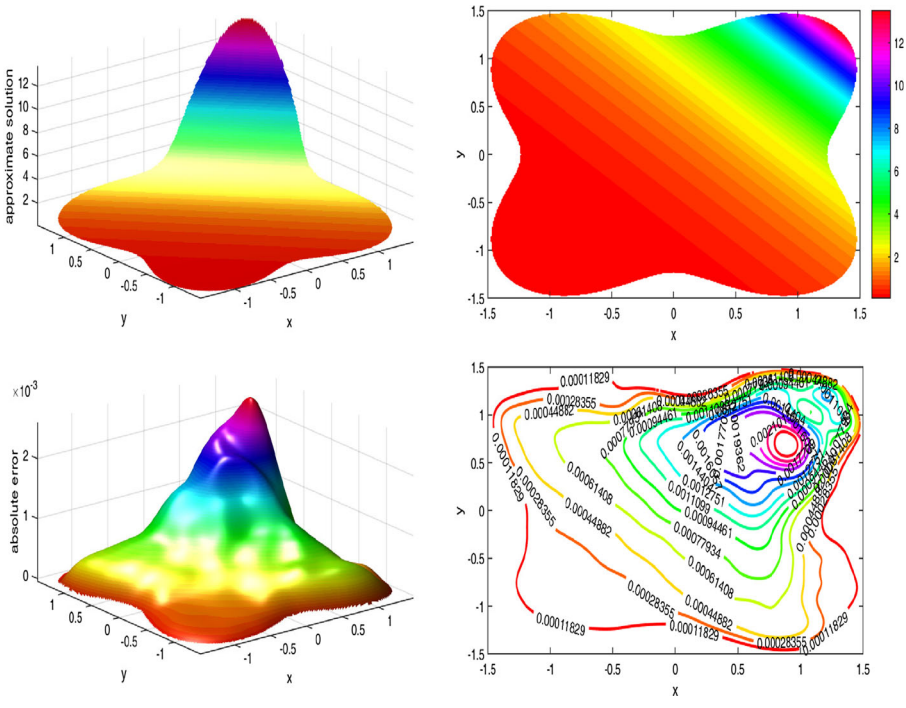

Fig. 8 Approximate solution and absolute error at $t = 1$ with $\alpha = 1.3$, $\alpha_1 = 1.1$ on Ω_1

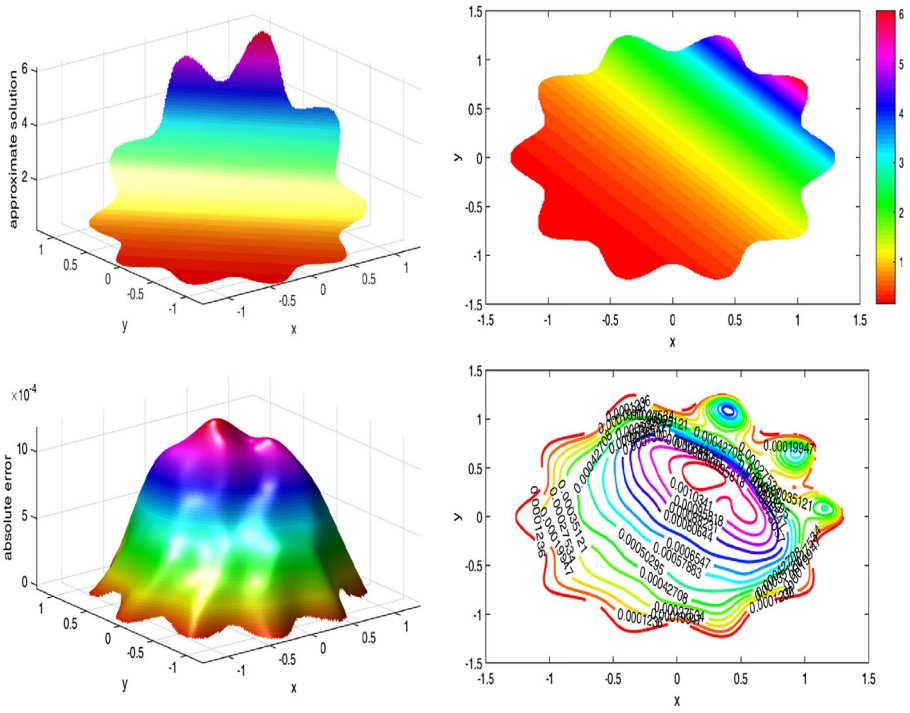

Fig. 9 Approximate solution and absolute error at $t = 1$ with $\alpha = 1.3,\ \alpha_1 = 1.1$ on Ω_2

Table 4 Absolute error and convergence rate associated with different time step-size for 1089 irregular nodal points on irregular domains with $\alpha = 1.3, \alpha_1 = 1.1$

Ω_1			Ω_2		
Step-size τ	L_∞	Ratio	Step-size τ	L_∞	Ratio
1/20	2.55917×10^{-2}	–	1/20	2.17967×10^{-2}	–
1/40	9.04967×10^{-3}	1.4997	1/40	8.46662×10^{-3}	1.3642
1/80	3.35596×10^{-3}	1.4311	1/80	3.15113×10^{-3}	1.4259
1/160	1.25706×10^{-3}	1.4167	1/160	1.17676×10^{-3}	1.4210

Table 5 CPU time in seconds for different geometries

	Problem domain			
N	Rectangular	Circular	Ω_1	Ω_2
64	0.593	0.590	0.686	0.645
256	6.081	5.115	5.108	5.298
1024	84.160	79.992	84.875	85.069
4096	1252.726	1198.275	1206.319	1200.95

5 Concluding remarks

In this study, a meshless point collocation method based on the MLSRK approximation is employed to solve the 2-D multi-term time fractional diffusion-wave equation. Strong form meshless methods are computationally efficient and easy to implement tools to model the real problems in science and engineering with reliable accuracy. We used a finite difference approximation to discretize the Caputo's time derivatives and obtained a semi-discrete scheme. Then, the unconditionally stability property and convergence of the resulted difference scheme are proved. Eventually, using the MLSRK approximation for spatial variables, a full discrete scheme is gained. To verify the theoretical outcomes, some test problems on rectangular, circular and complex domains with regular and irregular nodal points distribution are considered. From the obtained numerical solutions and errors, one can be seen that the proposed scheme is an efficient and reliable approach for the studied problem.

References

1. Abbaszadeh, M., Dehghan, M.: A meshless numerical procedure for solving fractional reaction–subdiffusion model via a new combination of alternating direction implicit (ADI) approach and interpolating element free Galerkin (EFG) method. Comput. Math. Appl. **70**, 2493–2512 (2015)
2. Atanackovic, T.M., Pilipovic, S., Zorica, D.: A diffusion wave equation with two fractional derivatives of different order. J. Phys. A: Math. Theor. **40**, 5319–5333 (2007)
3. Atluri, S.N., Shen, S.: The meshless local petrov-galerkin (mlpg) method. Technical Science Press, Encino, CA (2002)
4. Atluri, S.N., Shen, S.: The basis of meshless domain discretization: the meshless local Petrov-Galerkin (MLPG) method. Adv Comput. Math. **23**, 73–93 (2005)
5. Belystchko, T., Liu, Y.Y., Gu, L.: Element-free Galerkin methods. Int. J. Numer. Meth. Eng. **37**, 229–256 (1994)
6. Benson, D.A., Wheatcraft, S.W., Meerschaert, M.M.: Application of a fractional advection–dispersion equation. Water Resour. Res. **36**, 1403–1412 (2000)
7. Burrage, K., Hale, N., Kay, D.: An efficient implementation of an implicit FEM scheme for fractional-in-space reaction–diffusion equations. SIAM J. Sci. Comput. **34**, 2145–2172 (2012)
8. Chen, W., Pang, G.: A new definition of fractional Laplacian with application to modeling three-dimensional nonlocal heat conduction. J. Comput. Phys. **309**, 350–367 (2016)
9. Dehghan, M., Abbaszadeh, M., Mohebbi, A.: An implicit RBF meshless approach for solving the time fractional nonlinear sine–Gordon and Klein–Gordon equations. Eng. Anal. Bound. Elem. **50**, 412–434 (2015)
10. Dehghan, M., Abbaszadeh, M., Mohebbi, A.: Error estimate for the numerical solution of fractional reaction–subdiffusion process based on a meshless method. J. Comput. Appl. Math. **280**, 14–36 (2015)
11. Dehghan, M., Safarpoor, M., Abbaszadeh, M.: Two high-order numerical algorithms for solving the multi-term time fractional diffusion-wave equations. J. Comput. Appl. Math. **290**, 174–195 (2015)
12. Deng, W.: Finite element method for the space and time fractional Fokker–Planck equation. SIAM J. Numer. Anal. **47**, 204–226 (2008)
13. Diethelm, K., Ford, N.J.: Analysis of fractional differential equations. J. Math. Anal. Appl. **265**, 229–248 (2002)
14. Ding, X.L., Jiang, Y.L.: Analytical solutions for the multi-term time-space fractional advection–diffusion equations with mixed boundary conditions. Nonlin. Anal. RWA. **14**, 1026–1033 (2013)
15. Duarte, C.A., Oden, J.T.: H-p clouds—an h-p meshless method. Numer. Meth. Partial Diff. Eq. **12**, 673–705 (1996)
16. Du, R., Cao, W.R., Sun, Z.Z.: A compact difference scheme for the fractional diffusion–wave equation. Appl. Math. Model. **34**, 2998–3007 (2010)

17. Fu, Z.-J., Chen, W., Yang, H.-T.: Boundary particle method for Laplace transformed time fractional diffusion equations. J. Comput. phys. **235**, 52–66 (2013)
18. Fu, Z.-J., Chen, W., Ling, L.: Method of approximate particular solutions for constant- and variable-order fractional diffusion models. Engng. Anal. Bound. Elem. **57**, 37–46 (2015)
19. Gao, G., Sun, Z.Z.: A compact finite difference scheme for the fractional sub-diffusion equations. J. Comput. Phys. **230**, 586–595 (2011)
20. Gingold, R.A., Monaghan, J.J.: Smoothed particle hydrodynamics: theory and application to non-spherical stars. Mon. Not. R. Astr. Soc. **181**, 375–389 (1997)
21. Gorenflo, R., Mainardi, F., Scalas, E., Raberto, M.: Fractional calculus and continuous–time finance III: The diffusion limit. In: Mathematical Finance, pp. 171–80. Mathematics of Birkhauser, Basel (2001)
22. Gu, Y.T., Zhaung, P., Liu, F.: An advanced implicit meshless approach for the non-linear anomalous subdiffusion equation. Comput. Model. Eng. Sci. **56**, 303–333 (2010)
23. Han, W., Meng, X.: Error analysis of the reproducing kernel particle method. Comput. Meth. Appl. Mech. Eng. **190**, 6157–6181 (2001)
24. Hilfer, R.: Applications of fractional calculus in physics. World Scientific, Singapore (2000)
25. Jiang, Y., Ma, J.: High-order finite element methods for time fractional partial differential equations. J. Comput. Appl. Math. **235**, 3285–3290 (2011)
26. Jiang, H., Liu, F., Turner, I., Burrage, K.: Analytical solutions for the multi–term time fractional diffusion–wave/diffusion equations in a finite domain. Comput. Math. Appl. **64**, 3377–3388 (2012)
27. Jiang, H., Liu, F., Turner, I., Burrage, K.: Analytical solutions for the multi-term time–space Caputo–Riesz fractional advection–diffusion equations on a finite domain. J. Math. Anal. Appl. **389**, 1117–1127 (2012)
28. Jiang, H., Liu, F., Meerschaert, M.M., McGough, R.J., Liu, Q.: The fundamental solutions for multi-term modified power law wave equations in a finite domain. Electron. J. Math. Anal. Appl. **1**, 1–12 (2013)
29. Kansa, E.J.: Multiquadrics—a scattered data approximation scheme with applications to computational fluid dynamics. Comput. Math. Appl. **19**, 127–145 (1990)
30. Katsikadelis, J.T.: Numerical solution of multi-term fractional differential equations. J. Appl. Math. Mech. **89**, 593–608 (2009)
31. Kelly, J.F., McGough, R.J., Meerschaert, M.M.: Analytical time-domain Green's functions for power-law media. J. Acoust. Soc. Am. **124**, 2861–2872 (2008)
32. Kilbas, A.A., Srivastava, H.M., Trujillo, J.J.: Theory and applications of fractional differential equation. Elsevier, Amsterdam (2006)
33. Koeller, R.C.: Application of fractional calculus to the theory of viscoelasticity. J. Appl. Mech. **51**, 229–307 (1984)
34. Kwon, K.C., Park, S.H., Jiang, B.N., Youn, S.K.: The least-squares meshfree method for solving linear elastic problems. Comput. Mech. **30**, 196–211 (2003)
35. Liu, W.K., Jun, S., Zhang, Y.F.: Reproducing kernel particle methods. Inter. J. Numer. Meth. Flui. **20**, 1081–1106 (1995)
36. Liu, W.K., Li, S., Belytschko, T.: Moving least-square reproducing kernel methods (I) Methodology and convergence. Comput. Meth. Appl. Mech. Eng. **143**, 113–154 (1997)
37. Li, S., Liu, W.K.: Moving least square reproducing kernel method part II: Fourier analysis. Comput. Meth. Appl. Mech. Eng. **139**, 159–194 (1996)
38. Li, S., Liu, W.K.: Meshfree particle methods. Springer, Berlin (2007)
39. Liu, Q., Liu, F., Turner, I., Anh, V.: Finite element approximation for a modified anomalous subdiffusion equation. Appl. Math. Model. **35**, 4103–4116 (2011)
40. Liu, Q., Gu, Y.T., Zhuang, P., Liu, F., Nie, Y.F.: An implicit RBF meshless approach for time fractional diffusion equations. Comput. Mech. **48**, 1–12 (2011)
41. Liu, F., Meerschaert, M.M., McGough, R.J., Zhuang, P., Liu, Q.: Numerical methods for solving the multi-term time-fractional wave-diffusion equation. Fract. Calc. Appl. Anal. **16**, 9–25 (2013)
42. Liu, Q., Liu, F., Turner, I., Anh, V., Gu, Y.T.: A RBF meshless approach for modeling a fractal mobile/immobile transport model. Appl. Math. Comput. **226**, 336–347 (2014)
43. Liu, Q., Liu, F., Gu, Y.T., Zhuang, P., Chen, J., Turner, I.: A meshless method based on Point Interpolation Method (PIM) for the space fractional diffusion equation. Appl. Math. Comput. **256**, 930–938 (2015)

44. Lin, Y., Xu, C.: Finite difference/spectral approximation for the time–fractional diffusion equation. J. Comput. Phys. **225**, 1533–1552 (2007)
45. Luchko, Y.: Some uniqueness and existence results for the initial–boundary–value problems for the generalized time–fractional diffusion equation. Comput. Math Appl. **59**, 1766–1772 (2010)
46. Luchko, Y.: Initial-boundary-value problems for the generalized multi-term time–fractional diffusion equation. J. Math. Anal. Appl. **374**, 538–548 (2011)
47. Melenk, J.M., Babuska, I.: The partition of unity finite element method: basic theory and applications. Comput. Meth. Appl. Mech. Eng. **139**, 289–314 (1996)
48. Miller, K.S., Ross, B.: An introduction to fractional calculus and fractional differential equations (1974)
49. Meerschaert, M.M., Tadjeran, C.: Finite difference approximation for two-sided space–fractional partial differential equations. Appl. Numer. Math. **56**, 80–90 (2006)
50. Metzler, R., Klafter, J.: Boundary value problems for fractional diffusion equations. Phys. A **278**, 107–125 (2000)
51. Nayroles, B., Touzot, G., Villon, P.: Generalizing the finite element method: diffuse approximation and diffuse elements. Comput. Mech. **10**, 301–318 (1992)
52. Nigmatullin, R.R.: To the theoretical explanation of the universal response. Phys. Status (B): Basic Res. **123**, 739–745 (1984)
53. Nigmatullin, R.R.: Realization of the generalized transfer equation in a medium with fractal geometry. Phys. Status (B): Basic Res. **133**, 425–430 (1986)
54. Oldham, K.B., Spanier, J.: The fractional calculus: theory and application of differentiation and integration of arbitrary order. Academic Press, New York London (1974)
55. Oñate, E., Idelsohn, S., Zienkiewicz, O.C., Taylor, R.L., Sacco, C.: A finite point method for analysis of fluid mechanics problems. Applications to convective transport and fluid flow. Int. J. Numer. Meth. Eng. **39**, 3839–3866 (1996)
56. Pedas, A., Tamme, E.: Spline collocation methods for linear multi-term fractional differential equations. J. Comput. Appl. Math. **236**, 167–176 (2011)
57. Podlubny, I.: Fractional differential equations. Academic Press, San Diego (1999)
58. Raberto, M., Scalas, E., Mainardi, F.: Waiting-times and returns in high-frequency financial data: an empirical study. Phys. A **314**, 749–755 (2002)
59. Saadatmandi, A., Dehghan, M.: A tau approach for solution of the space fractional diffusion equation. Comput. Math. Appl. **62**, 1135–1142 (2011)
60. Scher, H., Montroll, E.: Anomalous transit-time dispersion in amorphous solids. Phys. Rev. B **12**, 24–55 (1975)
61. Schiessel, H., Metzler, R., Blumen, A., Nonnenmacher, T.F.: Generalized viscoelastic models: their fractional equations with solutions. J. Phys. A: Math. Gen. **28**, 6567–6584 (1995)
62. Srivastava, V., Rai, K.N.: A multi-term fractional diffusion equation for oxygen delivery through a capillary to tissues. Math. Comput. Model. **51**, 616–624 (2010)
63. Sun, Z.Z., Wu, X.N.: A fully discrete difference scheme for a diffusion-wave system. Appl. Numer. Math. **56**, 193–209 (2006)
64. Torvik, P.J., Bagley, R.L.: On the appearance of the fractional derivative in the behaviour of real materials. J. Appl. Mech. **51**, 294–298 (1984)
65. Wang, S., Zhang, H.: Partition of unity-based thermomechanical meshfree method for two-dimensional crack problems. Arch. Appl. Mech. **81**, 1351–1363 (2011)
66. Wei, L., He, Y.: Analysis of a fully discrete local discontinuous Galerkin method for time–fractional fourth-order problems. Appl. Math. Model. **38**, 1511–1522 (2014)
67. Yang, J.Y., Zhao, Y.M., Liu, N., Bu, W.P., Xu, T.L., Tang, Y.F.: An implicit MLS meshless method for 2-D time dependent fractional diffusion–wave equation. Appl. Math. Model. **39**, 1229–1240 (2015)
68. Ye, H., Liu, F., Anh, V., Turner, I.: Maximum principle and numerical method for the multi–term time–space Riesz–Caputo fractional differential equations. Appl. Math. Model. **227**, 531–540 (2014)
69. Zeng, F., Li, C., Liu, F., Turner, I.: The use of finite difference/element approaches for solving the time–fractional subdiffusion equation. SIAM. J. Sci. Comput. **35**, A2976–A3000 (2013)
70. Zeng, F., Liu, F., Li, C.P., Burrage, K., Turner, I., Anh, V.: A Crank–Nicolson ADI spectral method for a two-dimensional Riesz space fractional nonlinear reaction–diffusion equation. SIAM J. Numer. Anal. **52**, 2599–2622 (2014)

71. Zheng, M., Liu, F., Anh, V., Turner, I.: A high-order spectral method for the multi-term time–fractional diffusion equations. Appl. Math. Model. **40**, 4970–4985 (2016)
72. Zhuang, P., Gu, Y.T., Liu, F., Turner, I., Yarlagadda, P.K.D.V.: Time-dependent fractional advection–diffusion equations by an implicit MLS meshless method. Int. J. Numer. Meth. Eng. **88**, 1346–62 (2011)
73. Zhuang, P., Liu, F., Turner, I., Gu, Y.T.: Finite element methods for solving a one-dimensional space–fractional Boussinesq equation. Appl. Math Model. **38**, 3860–3870 (2014)